



## ENERGY-RELATED DEMANDS ON SEISMIC ISOLATORS IN BRIDGES

Gordon WARN<sup>1</sup> and Andrew WHITTAKER<sup>2</sup>

### SUMMARY

An analytical study investigating energy-related demands on individual seismic isolators in bridge structures subjected to earthquake excitation is summarized. Bidirectional nonlinear response-history analysis is employed considering a simple seismically isolated bridge model and three bins of earthquake ground motions. Properties of the idealized bilinear isolators, namely, the zero-displacement force-intercept and the second-slope period, are varied such that the results of this investigation are broadly applicable to seismically isolated bridge (and building) structures constructed in the United States. The results of these analyses are used to review the current American Association of State and Highway Transportation Officials (AASHTO) prototype testing requirements for seismic isolators under seismic loading conditions. This review suggests the current prototype testing requirements for seismic loading specified by AASHTO result in energy demands that are inconsistent with those determined from numerical simulation of maximum earthquake shaking. An improved prototype testing protocol for seismic isolators subjected to seismic loading is proposed.

### INTRODUCTION

The mechanical properties assumed in the design and analysis of the isolation system are checked prior to fabrication of production seismic isolators and installation in the bridge structure through prototype testing. Section 13.2 of the AASHTO Guide Specifications [1] include requirements for prototype testing of seismic isolators subjected to seismic loading, which include multiple cycles to the maximum design displacement,  $d$ . Specifically, the Guide Specifications in Section 13.2 write that a prototype isolator be subjected to (a) three fully reversed cycles at the following multiples of the total design displacement: 0.25, 0.5, 0.75, 1.0, 1.25, (b) not less than 10 and not more than 25 fully reversed cycles of loading at the design displacement,  $d$ , and (c) three fully reversed cycles of loading at the total design displacement, where the total design displacement is the design displacement plus a contribution due to torsion. A maximum speed (frequency) for testing is not specified in the AASHTO specifications and therefore these tests are typically conducted at slow speeds.

---

<sup>1</sup> Graduate Research Assistant, Department of Civil, Structural, and Environmental Engineering, University at Buffalo, Buffalo, NY 14260, USA. Email: warn@eng.buffalo.edu

<sup>2</sup> Associate Professor, Department of Civil, Structural, and Environmental Engineering, University at Buffalo, Buffalo, NY 14260, USA. Email: awhittak@eng.buffalo.edu

Presented in Fig. 1 is the force-displacement hysteresis from a lead-rubber (LR) bearing subject to 10 cycles of harmonic motion with displacement amplitude of 305 mm and a 0.5 Hz frequency [2]. After the first cycle the force response of the bearing is observed to decrease with each subsequent cycle with the response stabilizing around the 7th cycle. This behavior is typical of LR bearings and is due to heat generated in the lead core and temporary degradation of the strength of the core. However it is highly unlikely a seismic isolation bearing will be subjected to 10 fully reversed cycles to the design displacement during earthquake excitation. The results of this test provide potentially misleading information for the assessment of the prototype bearing and verification of values assumed in the design and analysis of the seismic isolation system. Accordingly, it is of significant import to bridge (and building) isolation construction that a prototype testing protocol be representative of the demand imposed on seismic isolators during maximum earthquake shaking.

The objective of this research study is to determine energy-related demands imposed on seismic isolators subjected to earthquake excitation and to translate these demands into an improved prototype testing protocol for seismic isolators subjected to seismic loading.

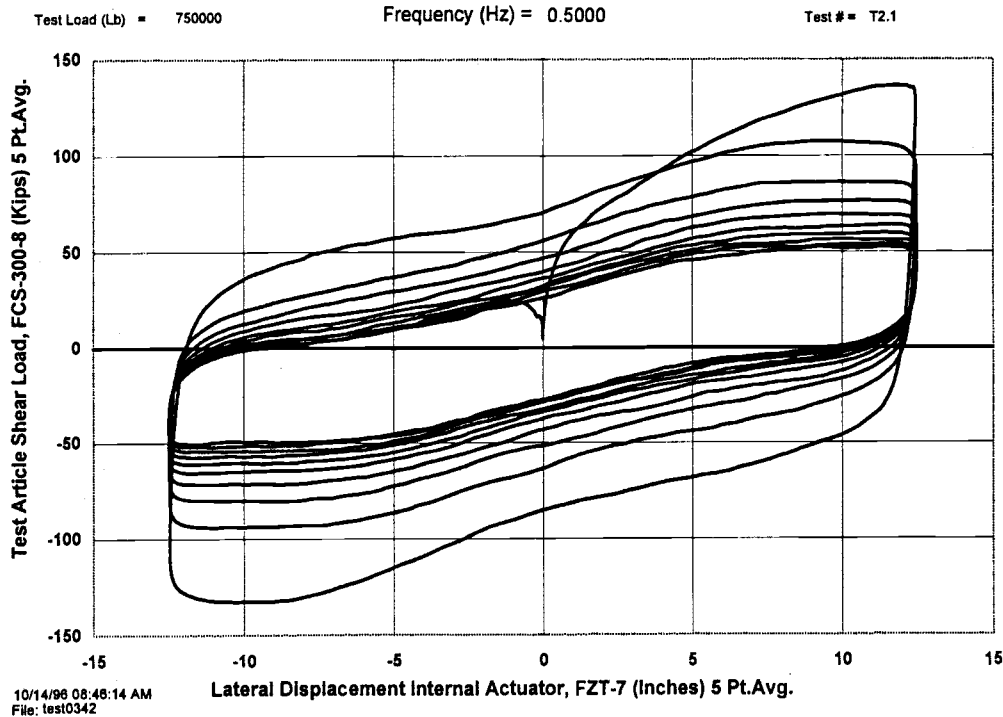


**Figure 1. Example test results for lead-rubber seismic isolator (HITEC, 1998)**

## TECHNICAL APPROACH

Response-history analysis is employed to determine the energy-related demands imposed on individual seismic isolation bearings during maximum earthquake shaking. A simple seismically isolated bridge structure is considered and subjected to bidirectional earthquake excitation. The seismic isolators are idealized using a bilinear force-displacement representation and modeled using a rate-independent coupled plasticity formulation, identical to formulations used by Huang et al. [3] and Mosqueda et al. [4].

Results of the response-history analyses conducted for this study were mined to provide new knowledge related to energy demands on seismic isolator and seismic isolation systems during maximum earthquake shaking. The force-displacement response of individual seismic isolator elements was numerically

integrated to determine the energy demand history. From this history, the total hysteretic energy demand and an estimated power demand were extracted. This information was used to review the current AASHTO prototype testing requirements for seismic isolators subjected to seismic loading [1] and to develop a prototype testing protocol representative of the energy demands imposed on seismic isolators during maximum earthquake shaking.

### Isolated bridge model

A mathematical model of a simple isolated bridge structure supported by four seismic isolators was assumed and implemented in Matlab [5] for the purposes of nonlinear response-history analysis. This model represents the simplest of isolated bridge structures and assumes both the superstructure and substructure to be rigid. Three degrees of freedom are used to describe the dynamic response of the isolated bridge, they are, two translational in the horizontal plane and one rotational about an axis perpendicular to the horizontal plane. Physical properties of the single-span superstructure were based on the middle span of a three-span example bridge structure set forth in a report by the Applied Technology Council (ATC) [6]. The bridge deck was assumed to be concrete resulting in a total deck weight of approximately 9900 kN. Each of the four seismic isolators is assumed to carry one quarter of the total deck weight (2475 kN). The center of mass is assumed to coincide with the center of rigidity of the isolation system in both horizontal and vertical planes, eliminating torsion and overturning moment caused by inertial forces.

The seismic isolators were modeled using a rate-independent coupled plasticity model [3, 4]. Parameters used for the coupled plasticity model are based on a bilinear characterization of the seismic isolators. This bilinear characterization and its defining parameters are shown in Fig. 2. Here  $Q_d$  is the zero-displacement force-intercept;  $K_u$  is the elastic stiffness;  $K_d$  is the second-slope stiffness;  $K_{eff}$  is the effective stiffness (peak-to-peak);  $d_y$  is the yield displacement assumed to be 0.25 mm for all isolation systems considered, typical of Friction Pendulum (FP) isolation bearings [7];  $d_{max}$  is the maximum displacement; and  $EDC$  is the energy dissipated in one fully reversed cycle to the maximum displacement shown by the area within the force-displacement loop. Note this characterization is similar to that assumed by the AASHTO Guide Specifications for Seismic Isolation Design [1].

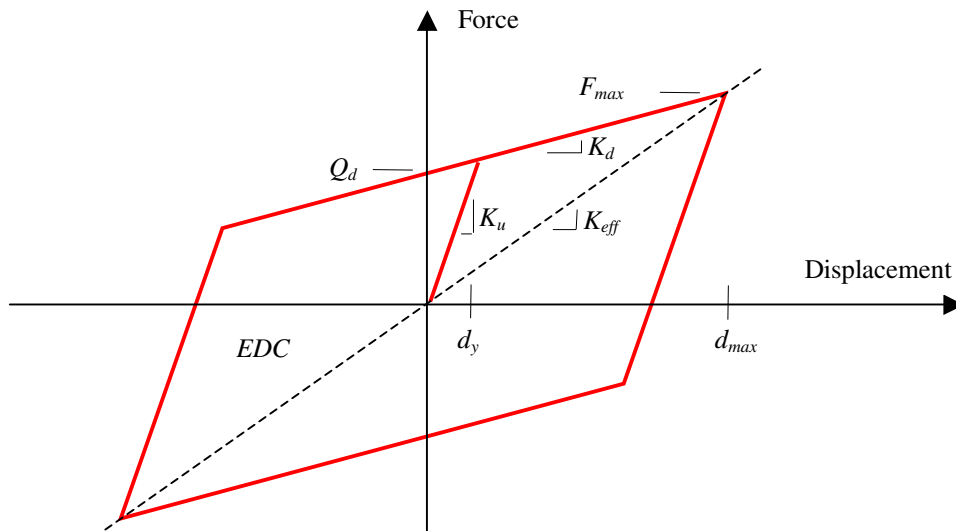


Figure 2. Idealized bilinear force-displacement relationship for a seismic isolator

Isolator parameters, specifically,  $Q_d$  and  $T_d$  (second-slope period) were varied widely to ensure the results of this study were applicable to the design of isolation systems in the United States. Twenty isolation systems were considered with  $T_d$  ranging from 1.5 to 4.0 seconds and  $Q_d/W$  (zero-displacement force-intercept normalized by the weight acting on the isolator) ranging from 0.03 to 0.12. Noting the second-slope period is related to the second-slope stiffness ( $K_d$ ) through the following expression

$$T_d = 2\pi \sqrt{\frac{W}{K_d g}} \quad (1)$$

where  $W$  is the weight acting on an individual isolator and  $g$  is the gravitational acceleration constant. Table 1 shows the range of isolator parameters considered. In this table each isolation system is identified using a three digit alpha-numeric naming system. For example, S33 denotes an isolation system with  $Q_d/W = 0.09$  and  $T_d = 2.5$  seconds. Typical bridge isolation systems are shown by the outlined region of the system matrix in Table 1, where  $Q_d/W$  ranges from 0.06 to 0.12 and  $T_d$  from 2.0 to 3.0 seconds.

**Table 1. Isolator parameter matrix**

		$T_d$ (seconds)				
		1.5	2.0	2.5	3.0	4.0
$Q_d/W$	0.03	S11	S12	S13	S14	S15
	0.06	S21	S22	S23	S24	S25
	0.09	S31	S32	S33	S34	S35
	0.12	S41	S42	S43	S44	S45

The response of the simple seismically isolated bridge model subjected to earthquake excitation was determined using Newmark's step-by-step integration procedure [8] implemented in Matlab [5]. Due to the assumed bilinear force-displacement relationship of the seismic isolator elements an iterative procedure is required at each time step. A modified Newton-Raphson procedure is used to determine the restoring force at each time step during the solution procedure. This numerical procedure is implicit and unconditionally stable [8] due to the choice of integration parameters,  $\gamma = 1/2$  and  $\beta = 1/4$ .

### Earthquake ground motions

A total of 72 pairs of earthquake ground motions were collected and organized into seven bins: an approach for organizing ground motions proposed by Krawinkler [9]. Information on all seven bins is provided in Warn [10]. Some of the results of response-history analysis using three of these bins (32 pairs) are presented in this paper. More information on these ground motion bins and corresponding results is also provided in Warn et al. [11]. All but six pairs of the acceleration histories were extracted from two sources: the Pacific Earthquake Engineering Research (PEER) database [12] and the SAC Steel Project database [13]. Six ground motion pairs were obtained from Miranda [14]. The ground motion bins are denoted: (1) Near-Field, (2M) Large-Magnitude, Small-Distance, and (7) Large-Magnitude, Soft-Soil. Summary information for ground motion pairs contained in each bin is presented in Table 2. This information includes: Number of Ground Motion Pairs, Moment Magnitude, Distance-to-Fault, Site Class and Classification system.

**Table 2. Ground motion bins**

Bin	Description	No. of Ground Motion Pairs	Moment Magnitude	Distance to Fault (km)	Site Class	Classification
1	NF	12	6.7 – 7.6	< 10	C / D	USGS/ NEHRP
2M	LMSD	10	6.5 – 7.3	10 – 30	A,B,C	USGS
7	LM-SS	10	6.9 – 8.1	2.6 – 385	E,F	USGS

Bin 1 (Near-Field) contains twelve pairs of earthquake ground motions, eight of which exhibit strong directivity effects, i.e., response from one component (fault normal) is significant greater than the response from the orthogonal component (fault parallel) for periods greater than 1.0-second. Ten pairs of ground motions contained in Bin 1 were classified with a soil type D as designated by the National Earthquake Hazard Reduction Program [15] corresponding to a stiff soil profile (average shear wave velocity ranging from 180-360 m/s). The remaining two pairs of ground motions were classified with a soil type C designated by the United States Geological Survey (USGS) corresponding to a stiff soil profile (average shear wave velocity ranging from 180-360 m/s) [12]. Ground motion pairs contained in Bin 2M represent large magnitude events with moment magnitude ranging from 6.5 to 7.3, distance-to-fault ranging from 10 km to 30 km and stiff soil or rock site conditions. Ground motions contained in Bin 2M were classified with soil type A, B or C as designated by USGS soil classification corresponding to rock (average shear wave velocity > 750 m/s), very dense soil or soft-rock (average shear wave velocity ranging from 360-750 m/s) and stiff soil (average shear wave velocity ranging from 180-360 m/s), respectively. Bin 7 is comprised of ground motions representing large magnitude events with moment magnitude ranging from 6.9 to 8.1 and soft-soil site conditions. Due to the limited number of large magnitude, the soft soil records distance-to-fault criteria was relaxed. Ground motions in Bin 7 are classified as either E or F per the NEHRP designation based on descriptions of local soil geology [16, 17]. Site class E represents soil profiles with soft clay layers greater than 3m in depth (average shear wave velocity < 180 m/s) [15]. Site class F represents soil profiles with soft organic clay layers greater than 3m in depth or soft clay layers with depth greater than 36 m [15]. Ground motion pairs contained in Bins 2M and 7 exhibited no clear directivity effects.

## RESULTS

Force-displacement response data determined from bidirectional nonlinear response-history analysis were utilized to determine energy-related demands imposed on seismic isolators during maximum earthquake shaking. The cumulative energy demand was determined by numerically integrating the force-displacement response and is denoted by Eq. (2)

$$E_T = \int F du \quad (2)$$

where  $F$  is the restoring force of the seismic isolator and  $du$  is an incremental displacement. The power demand placed on individual seismic isolator was estimated using Eq. (3) representing an average power demand based on 50-percent of the energy information.

$$R_E = \frac{0.75E_T - 0.25E_T}{t_{75} - t_{25}} \quad (3)$$

where  $0.75 E_T$  represents 75-percent of the total cumulative energy;  $0.25 E_T$  represents 25-percent of the total cumulative energy;  $t_{25}$  is the time corresponding to 25-percent of the total cumulative energy; and  $t_{75}$  is the time corresponding to 75-percent of the total cumulative energy. Fig. 3 shows a simple schematic of the power definition employed for this study. The energy history used in this figure is from the results of unidirectional response-history analysis using ground motion component RIO360 from the 1992 Cape Mendocino earthquake, Rio Dell Over Pass station (included in Bin 2M) with isolator properties  $Q_d / W = 0.06$  and  $T_d = 2.5$  seconds .

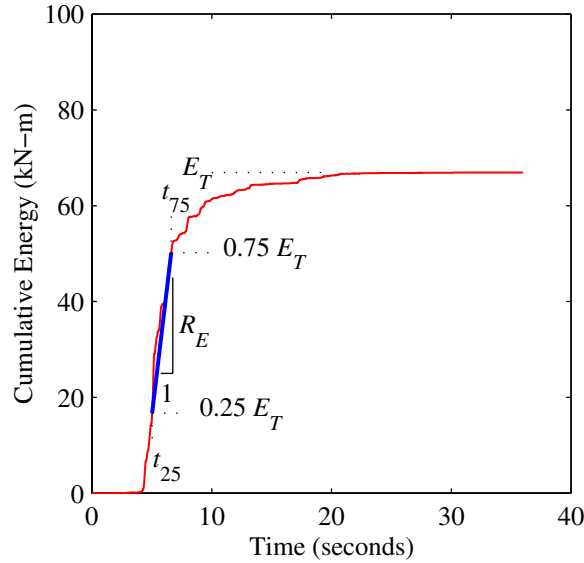


**Figure 3. Example energy history and defining energy demand parameters**

### Normalized energy demand

The total cumulative energy demand determined by integrating force-displacement response data was normalized by the energy dissipated in one fully reversed cycle to the maximum displacement (see Fig. 2). Normalizing the total energy demand by the  $EDC$  allows the results of this study to be generally applicable to isolators and isolation systems idealized using a bilinear force-displacement relationship and represents the number of harmonic cycles to the maximum displacement equivalent to the energy demand due to a severe earthquake. For bidirectional excitation the total cumulative energy demand is calculated as the sum of the total energy in the (horizontal)  $x$ - and  $y$ -directions. An expression for the normalized energy demand is given in Eq. (4)

$$NED = \frac{E_T}{EDC} \quad (4)$$

where  $E_T$  is the total energy defined previously and  $EDC$  is the energy dissipated from one fully reversed cycle to the maximum displacement. The  $EDC$  by a bilinear isolator (see Fig. 2) is calculated using Eq. 5 and was adopted from the AASHTO Guide Specifications [1]

$$EDC = 4Q_d (d_{max} - d_y) \quad (5)$$

where  $d_{max}$  is the maximum isolator displacement determined from response-history analysis and  $d_y$  is the yield displacement, assumed to be negligible for this calculation.

Normalized energy demand statistics determined from the results of bidirectional response-history analysis using ground motion pairs contained in Bin 1 are shown in Fig. 4. Fig. 4a presents mean (average) *NED* statistics plotted as a function of  $Q_d/W$  for each value of  $T_d$  considered. Mean information including sample standard deviation information is reproduced for isolation systems with  $T_d$  equal to 2.0 seconds in Fig. 4b. Sample standard deviation ( $\sigma$ ) information has been plotted to indicate the dispersion of *NED* data about the mean. Figs. 5 and 6 present *NED* statistics determined from the results of bidirectional response-history analysis using ground motion pairs contained in Bins 2M and 7, respectively. The presentation of Figs. 5 and 6 is identical to that of Fig. 4. In each of these figures, *NED* results, on average, are observed to decrease with increasing  $Q_d/W$  and  $T_d$ .

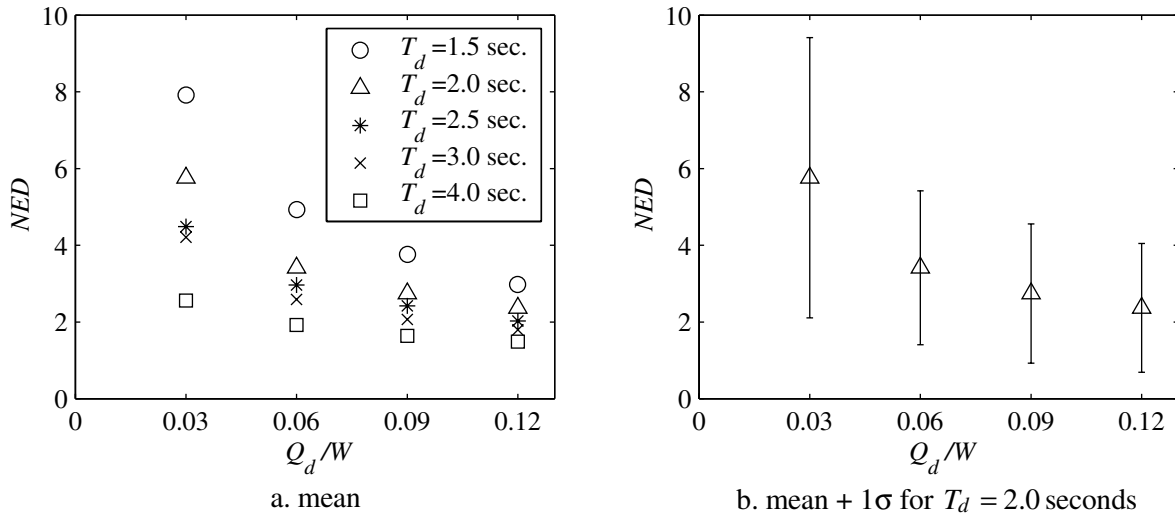


**Figure 4. Normalized energy demand statistics considering bidirectional excitation using ground motion pairs contained in Bin 1**

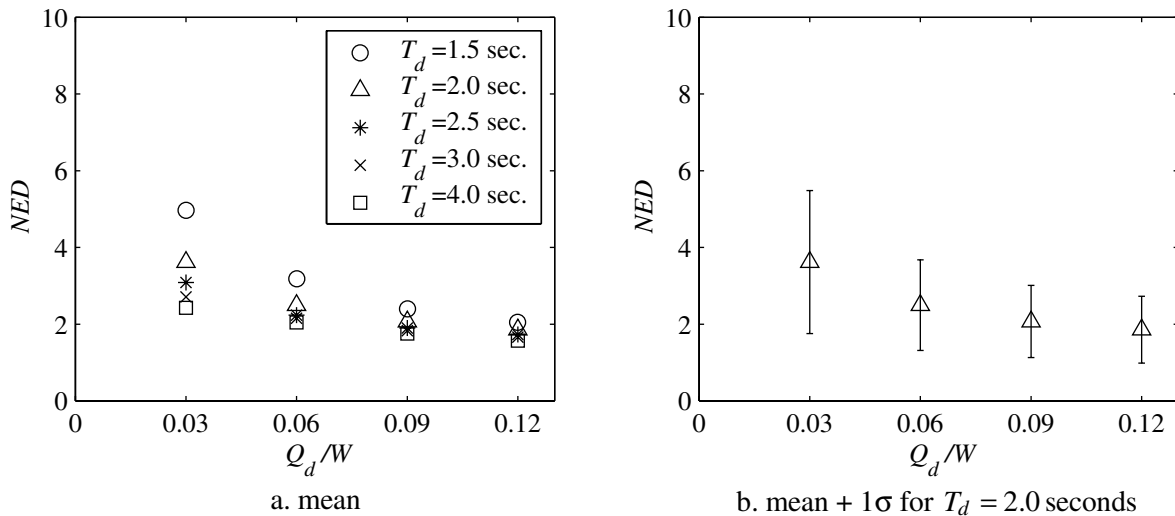


**Figure 5. Normalized energy demand statistics considering bidirectional excitation using ground motion pairs contained in Bin 2M**

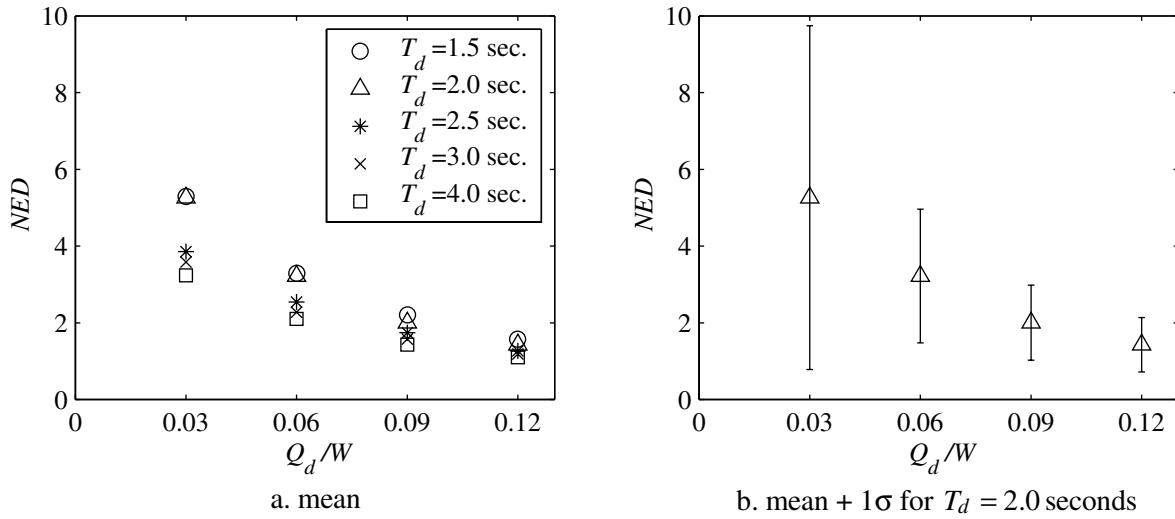


**Figure 6. Normalized energy demand statistics considering bidirectional excitation using ground motion pairs contained in Bin 7**

Mean and mean +  $1\sigma$  data calculated for Bins 1, 2M and 7 is re-plotted for all isolation systems with  $T_d = 2.0$  seconds in Fig. 7. Considering isolation systems with  $Q_d/W \geq 0.06$  (typical of bridge applications) it is observed that  $NED = 4.0$  (representing 4 fully reversed cycles to the maximum displacement) conservatively estimates mean total energy demands and  $NED = 5.0$  conservatively estimates mean +  $1\sigma$  energy demands for all three ground motion bins.

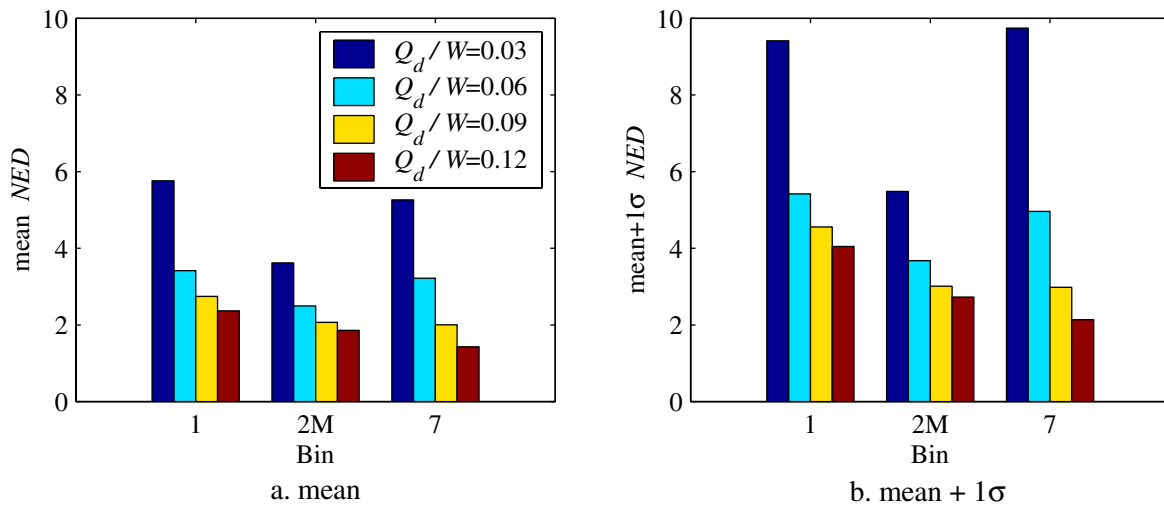


**Figure 7. Normalized energy demand statistics for ground motion bins 1, 2M and 7 for isolation systems with  $T_d = 2.0$  seconds**

### Equivalent frequency

An equivalent harmonic frequency is calculated using estimates of the power demand placed on individual seismic isolators ( $R_E$ ). This equivalent harmonic frequency is used to determine an appropriate frequency for prototype testing of seismic isolators. The equivalent harmonic frequency is calculated as

$$f_{eq} = \frac{R_E}{EDC} \quad (6)$$

where  $R_E$  is the mean estimated power demand defined previously and  $EDC$  is the energy dissipated in one fully reversed cycle to the maximum displacement calculated using Eq. (5) and the mean maximum isolator displacement determined from response-history analysis. Frequencies calculated using Eq. (6) were compared with an effective frequency determined using Eq. (7)

$$f_{eff} = \frac{1}{T_{eff}} \quad (7)$$

where  $T_{eff}$  is the effective period calculated from the effective stiffness,  $K_{eff}$ . Presented in Fig. 8 is a comparison of the calculated frequencies using Eq. (6) and Eq. (7), respectively, for ground motion bin 2M. In this figure the calculated frequencies are plotted as a function of  $Q_d/W$  for each value of  $T_d$  considered. Comparison of the frequencies presented in Fig. 8a ( $f_{eq}$ ) with those presented in Fig. 8b ( $f_{eff}$ ) suggest that a testing frequency based on the effective period (a parameter established in the design of the isolator system) conservatively estimates power demands placed on individual seismic isolators subjected to maximum earthquake shaking.

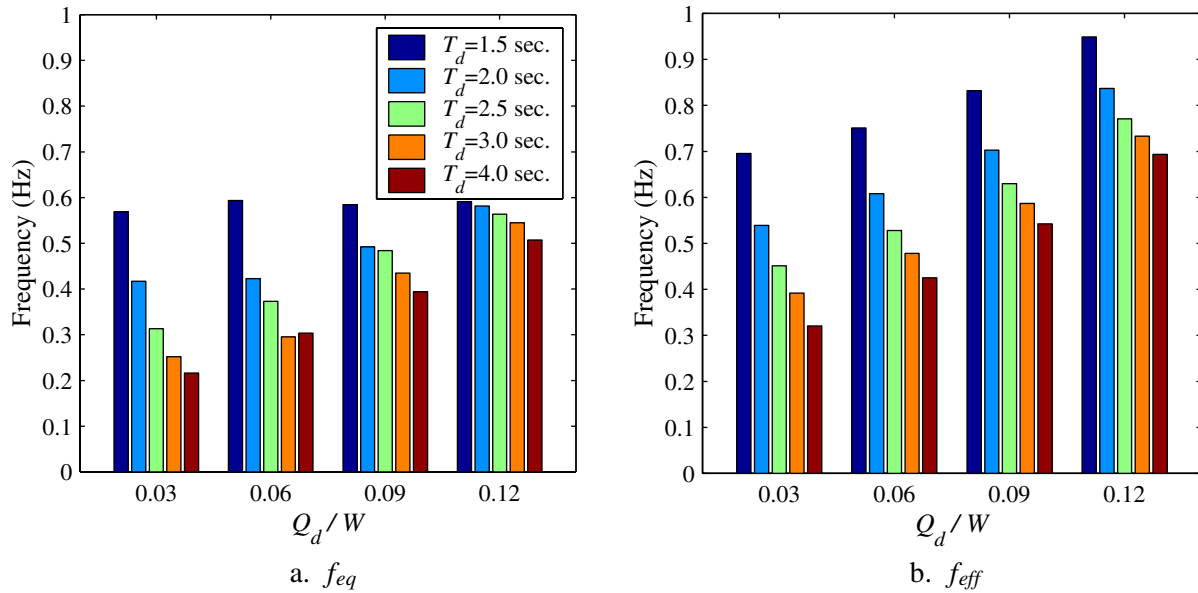


**Figure 8. Comparison of calculated frequencies based on the results of response-history analysis using ground motion pairs contained in Bin 2M**

## CONCLUSIONS AND RECOMMENDATIONS

The AASHTO Guide Specifications for Seismic Isolation Design [1] provide procedures for full-scale testing of seismic isolators. The results presented in this paper suggest the following. Total cumulative energy demands impose on individual seismic isolators determined from the results of numerical simulation of maximum earthquake shaking are far less than those imposed by the current AASHTO prototype testing protocol. The current testing protocol calls for 22 cycles to a displacement equal to or greater than the design displacement and 31 cycles of displacement to various amplitudes typically conducted at low maximum velocities.

Recommendations for the protocol testing of seismic isolators subjected to seismic loading include: 5 fully reversed cycles to the total design displacement at a frequency equal to  $1/T_{eff}$ , where the total design displacement includes the maximum isolator displacement plus a provision for an increase due to torsion, and  $T_{eff}$  is the effective period of the isolated structure.

### ACKNOWLEDGEMENTS

The authors gratefully acknowledge the financial support of the Multidisciplinary Center for Earthquake Engineering Research and the Federal Highway Administration through Task D1.3 of the Federal Highway Administration Contract DTFH 61-98-C-0094. The authors also wish to thank Professor Eduardo Miranda of Stanford University for contributing ground motion records for use in this study and Dr. Gilberto Mosqueda of the University of California at Berkeley for providing the Matlab code for the coupled plasticity model.

The opinions expressed in this paper are those of the writers and do not reflect the opinions of the Multidisciplinary Center for Earthquake Engineering Research or the Federal Highway Administration. No guarantee regarding the results, findings, and recommendations are offered by either the Multidisciplinary Center of Earthquake Engineering Research or the Federal Highway Administration.

### REFERENCES

1. American Association of State Highway Officials. *Guide Specifications for Seismic Isolation Design*, Washington, D.C., 1999.
2. Highway Innovative Technology Evaluation Center. *Evaluation Findings for Skellerup Base Isolation Elastomeric Bearings*, Technical Evaluation Report, CERF Report: #40369, 1998.
3. Huang W.H., Fenves G.L., Whittaker A.S., Mahin S.A. "Characterization of seismic isolation bearings for bridges from bi-directional testing". *Proceedings of the 12th World Conference on Earthquake Engineering*, 2000. p. 2047-2048.
4. Mosqueda G., Whittaker A.S., Fenves G.L. "Characterization and modeling of friction pendulum bearings subjected to multiple components of excitation". *Journal of Structural Engineering*, ASCE, 2003; accepted for publication.
5. MathWorks. Matlab. The Math Works, Inc. Natick, MA, 1999.
6. Applied Technology Council. *Seismic design guidelines for highway bridges*. Report 6. Redwood City, CA, 1986.
7. Mokha A.S., Constantinou M.C., Reinhorn A.M. "Verification of friction model of Teflon bearings under triaxial load". *Journal of Structural Engineering*, ASCE 1993; 119(1): 240-261.
8. Newmark N.M. "A method of computation for structural dynamics". *Journal of the Engineering Mechanics Division*, ASCE 1959; 85(3): 67-94.
9. Krawinkler. Private communication, 2001.
10. Warn G. "Performance estimates in seismically isolated bridge structures". M.S. Thesis, University at Buffalo, NY, 2003.
11. Warn G., Whittaker A. "Performance estimates in seismically isolated bridge structures". *Engineering Structures*, 2004; accepted for publication.
12. Pacific Earthquake Engineering Research. Strong Motion Database. <http://peer.berkeley.edu/smcat/>, 2000.
13. SAC Steel Project. Suites of earthquake ground motions for analysis of steel moment frame structures, [http://nisee.berkeley.edu/data/strong\\_motion/sacsteel/ground\\_motions.html](http://nisee.berkeley.edu/data/strong_motion/sacsteel/ground_motions.html), 1997.
14. Miranda. Private communication, 2002.

15. National Earthquake Hazard Reduction Program. *Recommended provisions for seismic regulations for new buildings and other structures, Part-1*. Building Seismic Safety Council for the Federal Emergency Management Agency, Washington. D.C., 2001.
16. Benuska L “Loma Prieta earthquake reconnaissance report.” *Earthquake Spectra*, sup. vol. 6, EERI 1990. p. 25-80.
17. Miranda E “Seismic evaluation and upgrading of existing buildings.” Ph.D. Thesis, University of California, Berkeley, CA, 1991.